DOCUMENT NUMBER 67SD289
AUGUST 1, 1967

ENVIRONMENTAL PRESSURES ON SATELLITES

PREPARED FOR

NATIONAL AERONAUTICS AND SPACE ADMINISTRATION
MARSHALL SPACE FLIGHT CENTER
HUNTSVILLE, ALABAMA

UNDER NASA CONTRACT NO. NAS-8-21043

GENERAL ELECTRIC
SPACECRAFT DEPARTMENT
A Department of the Missile and Space Division
Valley Forge Space Technology Center
P. O. Box 8555 • Philadelphia, Penna. 19101

TABLE OF CONTENTS

LIST OF ILLUSTRATIONS

ACKNOWLEDGEMENTS

The author expresses his appreciation to J. R. Freelin, R. E. Roach, and B. Wilcox for helpful suggestions, and to the authors of the reports listed among the references for their important basic work.

SUMMARY

The equations and logic used for the digital computer simulation of environmental pressure effects on an earth-orbiting satellite are presented. Although they were derived for use with the flexible body structural dynamical simulation, they are equally applicable to any combination of rigid, articulated, and flexible bodies, within the limitations described.

The environmental pressures analyzed here include solar radiation, aerodynamic, and earth's albedo pressures. All of these effects involve a pressure due to exchange of momentum between the satellite and an incident flux of particles or photons. Therefore, the mathematical models for their effects are analogous. Because of this, the same equations can be used for force and torque in each analysis. This is a great economy in the engineering analysis, programming effort, and checkout of the program, but probably does not affect computer running time appreciably.

The scheme for combining the simulation of the three effects is explained by referring to the logic chart of Figure 1. The inclusion of any effect in a particular computer run is an option of the user. If the choice is to include an effect, it is still excluded under particular circumstances, as indicated in the chart. For each of the effects, the computations peculiar to that effect are performed first. Then a common set of equations and logic is used for shadow geometry, forces, and torques.

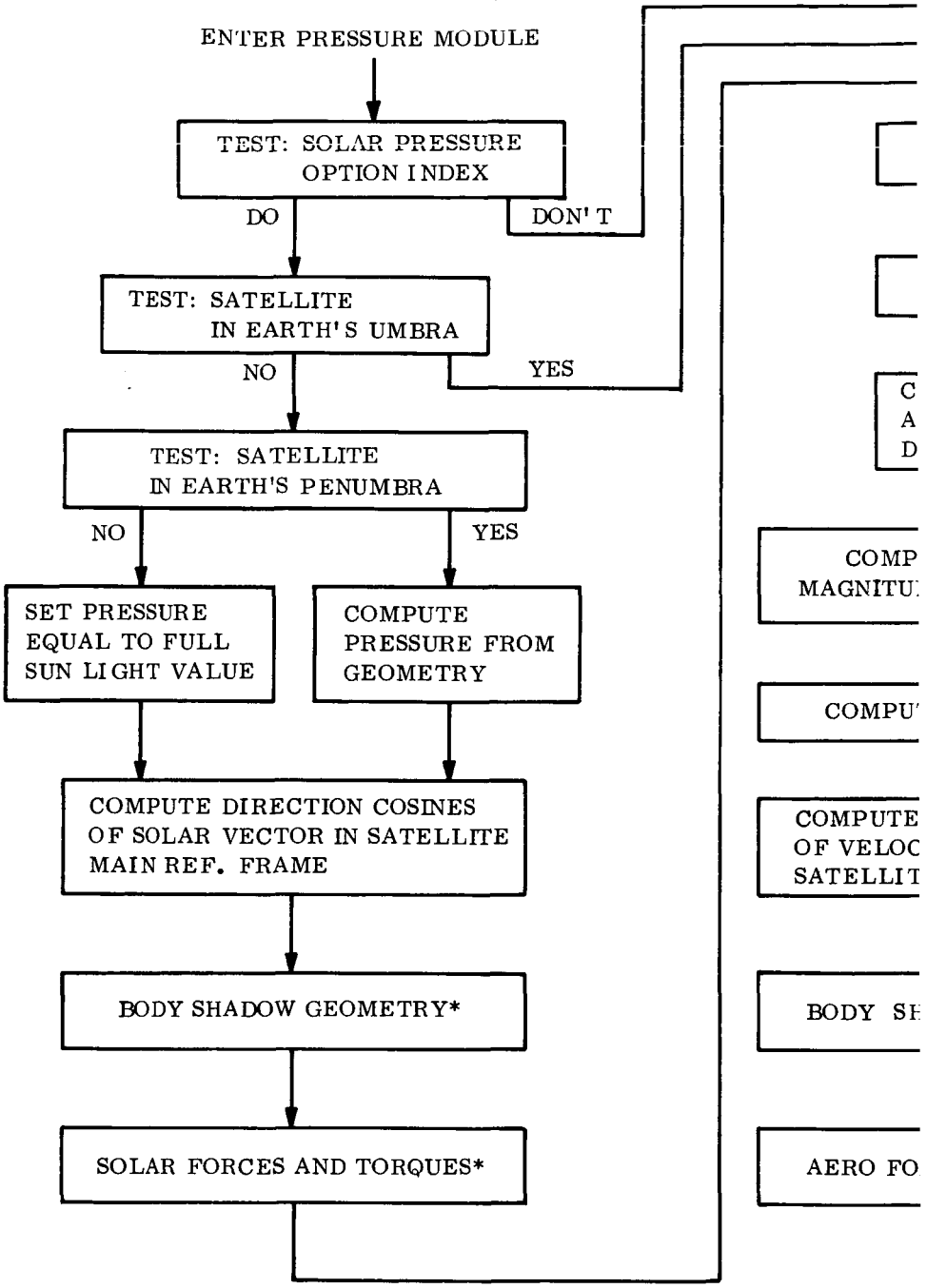

*ALL SHADOW GEOMETRY MODULES ARE IDENTICAL, AND ALL MODULES ARE IDENTICAL FOR SOLAR RADIATION, AERODYNA PRESSURES

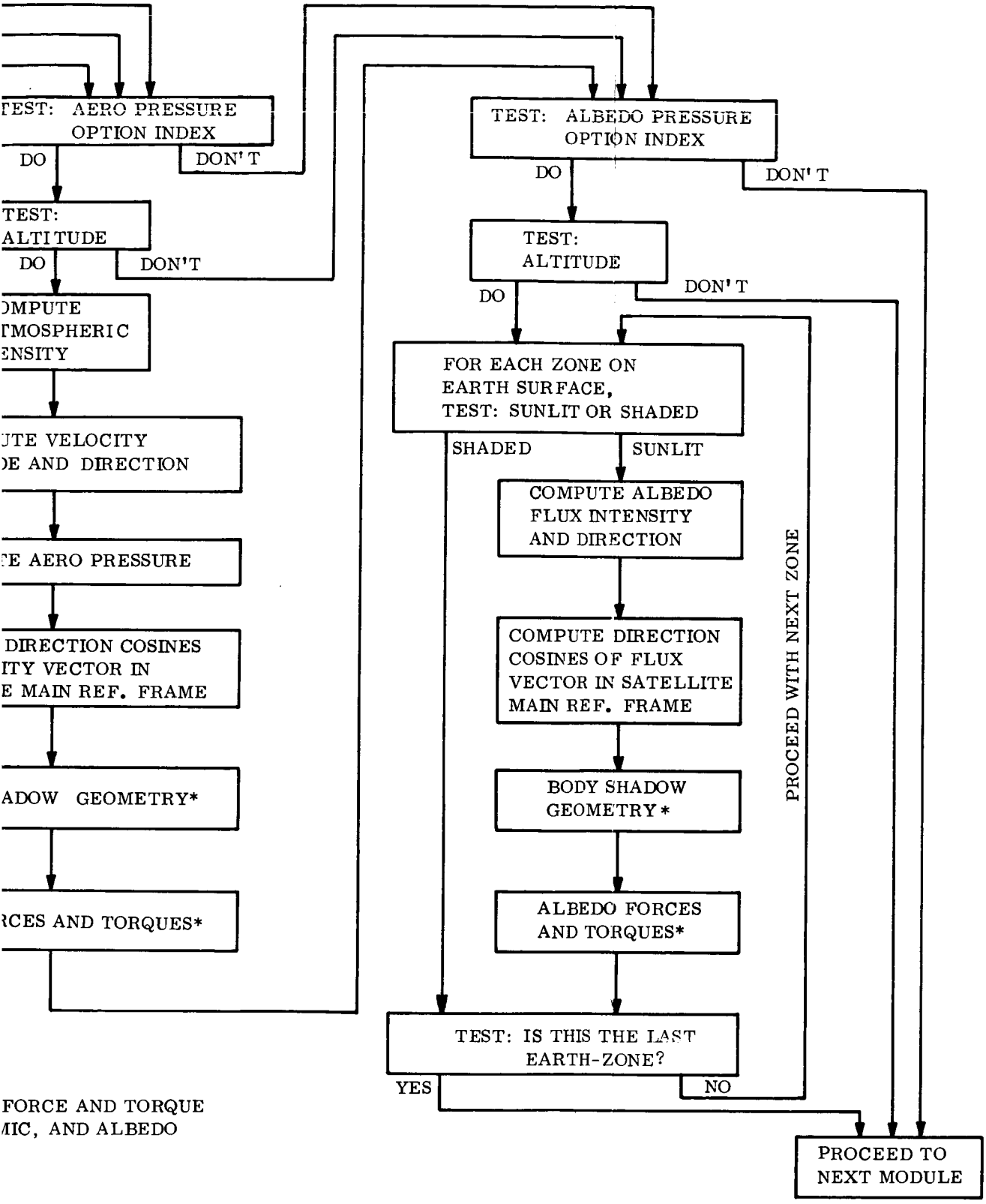

Figure 1. Environmental Pressure Module

SECTION 1

INTRODUCTION

The simplified analyses of satellite body shadows and of earth's albedo effects were performed under Contract No. NAS-8-21043 with NASA-Marshall Space Flight Center, Huntsville, Alabama. This contract was awarded to the General Electric Company's Spacecraft Department for studying the dynamics of an elastic spacecraft. The interactions of structural dynamics, attitude dynamics, and orbital dynamics are of special interest.

The analyses of aerodynamic and solar radiation pressure effects were largely part of the in-house effort in making digital simulations of passively oriented systems. Only such results as are peculiar to the present contract are included here. The more basic work is described in various reports which are referenced throughout this document.

SECTION 2

SOLAR RADIATION PRESSURE

The computation of solar forces and torques takes into account the apparent sun position, the reduction of solar flux in the earth's penumbra, the absence of flux in the umbra, the surface characteristics of various parts of the satellite, structural deflections, and the effects of complete or partial shading of one part of the satellite by another.

The unit vector in the direction of the solar flux is designated $\bar{S}$. The components of $\bar{S}$ in the $\bar{X}_o \bar{Y}_o \bar{Z}_o$ orbital frame and in the $\bar{X}_m \bar{Y}_m \bar{Z}_m$ satellite frame are known at any instant as components of a state vector. The satellite is in the earth's umbra if

$$\bar{S} \cdot \bar{X}_O \geqq \frac{R_E (R_S - R_E)}{R_{SE} R_O} + \sqrt{1 - \left(\frac{R_E}{R_O}\right)^2} \sqrt{1 - \left(\frac{R_S - R_E}{R_{SE}}\right)^2} \qquad (2\text{-}1)$$

where:

R_E is the earth's radius,

R_S is the sun's radius,

R_{SE} is the distance from the heliocenter to the geocenter,

R_O is the geocentric distance of the satellite.

If the satellite is in the earth's umbra, the solar forces and torques are all equal to zero.

The satellite is in full sunlight if

$$\bar{S} \cdot \bar{X}_O \leqq \sqrt{1 - \left(\frac{R_E}{R_O}\right)^2} \sqrt{1 - \left(\frac{R_S + R_E}{R_{SE}}\right)^2} - \frac{R_E (R_S + R_E)}{R_{SE} R_O} \qquad (2\text{-}2)$$

In this case, the solar pressure, P_S, is 9.53×10^{-8} pounds per square foot, or 4.56×10^{-5} dynes per square centimeter.

If neither of the above conditions holds, the satellite is in the earth's penumbra. The intensity is computed from the following equations which are simplified versions of those in Section 4 of Reference 1.

$$\sin \psi = \frac{R_E}{R_O} \quad , \tag{2-3}$$

$$\cos \mu = \bar{S} \cdot \bar{X}_O, \tag{2-4}$$

$$\sin \beta_{min} = \frac{1}{R_S} \left[R_E - (R_{SE} - R_S) \sin (\mu - \psi) \right] , \tag{2-5}$$

The intensity is then

$$P_S = P_O \left[\frac{1}{2} - \frac{1}{\pi} (\beta_{min} - \sin \beta_{min} \cos \beta_{min}) \right] ,$$

where P_O has the numerical value given previously, for P_S, and β_{min} is a positive or negative acute angle.

The computation of solar radiation pressure forces and torques is described in Section 6.

SECTION 3

AERODYNAMIC PRESSURE

The computation of aerodynamic forces and torques takes into account the relative wind velocity, the variation of atmospheric density with geodetic altitude, the surface characteristics of various parts of the satellite, structural deflections, and the effects of complete or partial shielding of one part of the satellite by another.

The analysis is based on free flow, and is therefore valid only at altitudes of about 200 kilometers or higher. The atmospheric density model is based on the work of Jacchia, as reported in Reference 2. The equations for the atmospheric density, in the foot-pound-second system, are given in Sections 17.2 and 17.3 of Reference 3.

The relative wind velocity, satellite altitude, attitude, latitude, and structural deflections are known at any instant as components of a state vector.

The aerodynamic pressure is

$$P_A = \rho_A V^2, \tag{3-1}$$

where ρ_A is the atmospheric density and V is the relative wind velocity. This equation is derived in Section 17.3 of Reference 3, and the basic assumptions are stated there.

The computation of aerodynamic forces and torques is analogous to that of solar forces and torques, as described in Section 6.

SECTION 4

ALBEDO PRESSURE

The computation of albedo forces and torques takes into account all of the factors which affect solar forces and torques and, in addition, the geometry and characteristics of that portion of the earth's surface which is both illuminated by the sun and visible from the satellite. The major differences between the albedo pressure and solar radiation pressure are: (1) the albedo flux comes from various directions while the solar flux comes from a single direction, and (2) the albedo flux varies in intensity while the solar flux is practically constant whenever the sun is completely visible. The varying direction and magnitude of the albedo flux complicate the analysis of its effects on the spacecraft. To keep the analysis economical and usable, some gross approximations are made. These are applicable to large digital computer solution, and may be refined at a future date to obtain better accuracy at the cost of greater computer running time, without modifying the basic analysis.

The approach taken is to divide into zones that portion of the earth's surface which is visible from the satellite. If a particular zone is sunlit, then it acts as a reflector, sending flux to the satellite. The flux from each zone is considered parallel, and of an intensity corresponding to the total value for that zone. The effect on the satellite of the flux from each zone is then computed in the same manner as the effect of the solar flux. Such effects include forces and torques or their absence at particular locations because of body shadows.

For convenience in computing the albedo flux vector at the satellite, a reference frame described by the $\bar{X}_A \bar{Y}_A \bar{Z}_A$ orthonormal triad is used. The $\bar{X}_A \bar{Y}_A$ plane contains the sun, the earth, and the satellite. The $\bar{X}_A$ unit vector coincides with the $\bar{X}_O$ unit vector, and the $\bar{Y}_A$ unit vector is such that the solar flux has a positive $\bar{Y}_A$ component. The $\bar{Z}_A$ unit vector forms a right-handed system.

The rotational transformation from the orbital reference frame to the albedo reference frame is

$$\begin{bmatrix} \bar{X}_A \\ \bar{Y}_A \\ \bar{Z}_A \end{bmatrix} = \left[A_4\right] \begin{bmatrix} \bar{X}_O \\ \bar{Y}_O \\ \bar{Z}_O \end{bmatrix} \tag{4-1}$$

where

$$\left[A_4\right] \begin{bmatrix} 1 & 0 & 0 \\ 0 & \dfrac{S_{YO}}{\sqrt{S_{YO}^2 + S_{ZO}^2}} & \dfrac{S_{ZO}}{\sqrt{S_{YO}^2 + S_{ZO}^2}} \\ 0 & -\dfrac{S_{ZO}}{\sqrt{S_{YO}^2 + S_{ZO}^2}} & \dfrac{S_{YO}}{\sqrt{S_{YO}^2 + S_{ZO}^2}} \end{bmatrix}, \tag{4-2}$$

and S_{XO}, S_{YO}, S_{ZO} are the direction cosines of the solar flux vector in the orbital reference frame. If the solar flux is parallel to $\bar{X}_O$, then the albedo reference frame is undefined, but it is not needed. In this case, the $\left[A_4\right]$ matrix is set equal to the identity matrix for convenience.

The components of the solar flux unit vector in the albedo reference frame are computed from

$$\begin{bmatrix} S_{XA} \\ S_{YA} \\ S_{ZA} \end{bmatrix} = \left[A_4\right] \begin{bmatrix} S_{XO} \\ S_{YO} \\ S_{ZO} \end{bmatrix} \tag{4-3}$$

from which

$$S_{XA} = S_{XO} \tag{4-4}$$

$$S_{YA} = +\sqrt{S_{YO}^{2} + S_{ZO}^{2}}, \tag{4-5}$$

$$S_{ZA} = 0. \tag{4-6}$$

The geometry of the albedo analysis is partially illustrated by Figure 4-1. The portion of the earth's surface seen from the satellite has cylindrical symmetry about the $\bar{X}_A$ axis. The surface is divided into annular surfaces, which are further subdivided into zones, as shown in Figure 4-1. The average value, over the I^{th} annulus, of the declination angle β, measured from the $\bar{X}_A$ axis, is β_{CI}. The average value of the azimuth angle ϕ in the J^{th} segment of the I^{th} annulus is ϕ_{CIJ}. Then the unit vector pointing from the geocenter to the center of this IJ^{th} surface zone is

$$\bar{R} = \bar{X}_A \cos\beta_{CI} + \bar{Y}_A \sin\beta_{CI} \cos\phi_{CIJ} + \bar{Z}_A \sin\beta_{CI} \sin\phi_{CIJ}. \tag{4-7}$$

The cosine of the angle of incidence of solar rays at the center of the IJ^{th} zone is

$$\bar{S} \cdot (-\bar{R}) = S_{XA} \cos\beta_{CI} + S_{YA} \sin\beta_{CI} \cos\phi_{CIJ}. \tag{4-8}$$

If the right-hand member of this equation is positive, the center of the zone is sunlit. Therefore, the entire zone is considered sunlit. Otherwise, it is considered shaded.

If the zone is sunlit, the magnitude and direction of the albedo flux reflected from the area to the satellite are computed (as described later). If the zone is shaded, all computations for that zone are omitted (for the present time interval).

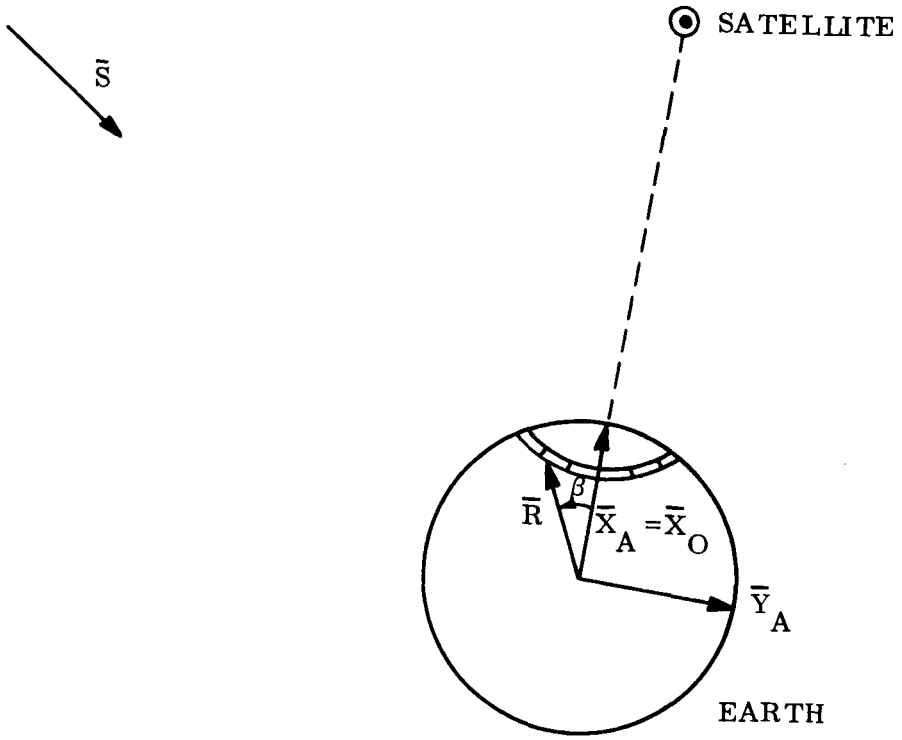

Figure 4-1. Albedo Geometry

A systematic method for determining and designating the zones on the earth's surface is required. The number of annular rings (such as the one illustrated in Figure 4-1) is N_B. This number controls the mesh fineness and therefore, the accuracy of the albedo analysis. The outer boundary of the last ring corresponds to the edge of the region visible from the satellite. The value of β corresponding to this boundary is computed from

$$\cos \beta_{Max} = \frac{R_E}{R_O}. \tag{4-9}$$

In order to divide the visible portion of the earth's surface into equal areas, each annulus, except the first, is subdivided as explained below. The first annulus is a circle whose center is at the subsatellite point.

The range of β within each annulus is

$$\Delta \beta = \frac{2 \beta_{Max}}{2N_B - 1} \tag{4-10}$$

Figure 4-2 illustrates the case where N_B is three. In this case, the second annulus is subdivided into eight equal segments, and the third is subdivided into sixteen equal segments.

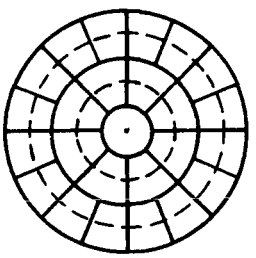

Figure 4-2. Zone Geometry

The ratio of the area of the whole visible region to that of the center circle is

$$(2N_B - 1)^2 \tag{4-11}$$

The ratio of the projected area of the Ith ring to that of the center circle is

$$N_{AI} = (2I - 1)^2 - (2I - 3)^2 = 8 (I - 1). \tag{4-12}$$

This is also the number of segments in the I_{th} ring, such that each has the same area as the center circle. The average value of β for the I_{th} ring is

$$\beta_{CI} = \Delta\beta (I - 1). \tag{4-13}$$

These average values of β correspond to the dashed circles in Figure 4-2. Table 4-1 lists the relations for any number of rings up to six. The semi-range of β within each ring is

$$\beta_R = \frac{1}{2} \Delta\beta. \tag{4-14}$$

Table 4-1. Annulus Parameters

Number of Rings, N_B	2	3	4	5	6
$\frac{\Delta\beta}{\beta_{Max}}$	$\frac{2}{3}$	$\frac{2}{5}$	$\frac{2}{7}$	$\frac{2}{9}$	$\frac{2}{11}$
Area ratio of entire area	9	25	49	81	121
Area ratio, N_A, of outer annulus	8	16	24	32	40

The segments of each annulus are numbered beginning at the $\bar{Y}_A$ axis and continuing toward the $\bar{Z}_A$ axis. For the J^{th} segment in the I^{th} ring, the center value of the azimuth angle, ϕ, is

$$\phi_{CIJ} = \frac{\pi\,(2J - 1)}{N_{AI}} \tag{4-15}$$

The semi-range of ϕ within each segment is

$$\phi_{RI} = \frac{\pi}{N_{AI}} \tag{4-16}$$

The geocentric coordinates of any zone on the earth's surface lie within the following ranges:

$$\beta_{CI} - \beta_R \leqq \beta \leqq \beta_{CI} + \beta_R, \tag{4-17}$$

$$\phi_{CIJ} - \phi_{RI} \leqq \phi \leqq \phi_{CIJ} + \phi_{RI}. \tag{4-18}$$

The magnitude at the satellite of the albedo pressure, due to reflection from the IJ^{th} zone, is P_{AIJ}. The direction cosines of this vector flux, in the albedo reference frame, are A_{AIJ}, B_{AIJ}, and C_{AIJ}. These are all computed as described later. The direction cosines in the satellite main reference frame are computed from

$$\begin{bmatrix} A_{MIJ} \\ B_{MIJ} \\ C_{MIJ} \end{bmatrix} = \begin{bmatrix} A_4 \end{bmatrix}^T \begin{bmatrix} A_{AIJ} \\ B_{AIJ} \\ C_{AIJ} \end{bmatrix} \tag{4-19}$$

where T indicates the tranpose of the matrix.

The computation of the albedo flux from the IJ^{th} zone will now be described. The derivation follows the general method of Reference 4.

The intensity of the incident solar flux at any sunlit point on the earth's surface, expressed as a pressure, is P_s multiplied by either member of Equation 4-8. The area of any surface element is

$$dA_G = R_E^2 \sin\beta \, d\beta \, d\phi \tag{4-20}$$

The total flux reflected from this area element is $d^2F_E = A_E P_S R_E^2 \sin\beta \, \bar{S} \cdot (-\bar{R}) \, d\beta \, d\phi$, where A_E is the earth's albedo, approximately 0. 34.

The flux density at the satellite is computed with the aid of the vector diagram of Figure 4-3. The geocentric distance of the satellite is R_o. The vector from the earth surface element to the satellite is

$$\vec{Q} = \bar{X}_A R_O - \bar{R} R_E$$

$$= \bar{X}_A (R_O - R_E \cos \beta)$$

$$-\bar{Y}_A R_E \sin \beta \cos \phi$$

$$-\bar{Z}_A R_E \sin \beta \sin \phi \qquad (4\text{-}21)$$

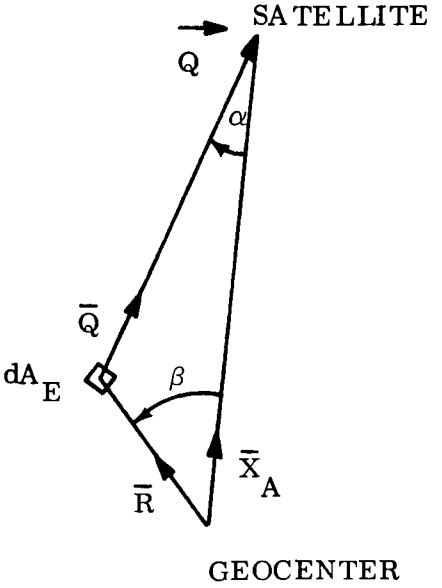

Figure 4-3. Albedo Geometry, Vector Diagram

The magnitude of this vector is

$$Q = \sqrt{\vec{Q} \cdot \vec{Q}} = \sqrt{R_O^2 + R_E^2 - 2 R_O R_E \cos \beta}. \qquad (4\text{-}22)$$

The unit vector along $\vec{Q}$ is

$$\bar{Q} = \frac{\vec{Q}}{Q} \qquad (4\text{-}23)$$

For Lambert Law reflection, the flux at any point along $\vec{Q}$, impinging on an area which subtends a solid angle $d\Omega$, is

$$d^4 P_A = \frac{1}{\pi} (\bar{R} \cdot \bar{Q})\, d^2 F_E\, d\Omega \qquad (4\text{-}24)$$

For a unit area at the satellite,

$$\Omega = \frac{1}{Q^2}, \tag{4-25}$$

replaces $d\Omega$. Also,

$$\bar{R} \cdot \bar{Q} = \frac{1}{Q} \; \bar{R} \cdot \vec{Q} = \frac{1}{Q} \; (R_o \cos \beta - R_E). \tag{4-26}$$

The vector flux density at the satellite, expressed as a pressure, is Equation 4-24 multiplied by the unit vector $\bar{Q}$.

$$\vec{d^2 P_A} = \frac{P_S A_E R_E^2}{\pi Q^4} \sin \beta \, (R_O \cos \beta - R_E) \, (S_{XA} \cos \beta + S_{YA} \sin \beta \cos \phi)$$
$$\cdot \left[\bar{X}_A \, (R_O - R_E \cos \beta) - \bar{Y}_A R_E \sin \beta \cos \phi - \bar{Z}_A R_E \sin \beta \sin \phi \right] d\beta \, d\phi. \tag{4-27}$$

The last two factors are the only ones which are functions of ϕ. These are multiplied together, and the result is integrated with respect to ϕ over the range given by Equation 4-18. It is convenient to define the following integrals as functions of ϕ_{CIJ} and of ϕ_{RI}:

$$F_{1IJ} = \int d\phi = 2 \phi_{RI}, \tag{4-28}$$

$$F_{2IJ} = \int \sin \phi \, d\phi = 2 \sin \phi_{CIJ} \sin \phi_{RI}, \tag{4-29}$$

$$F_{3IJ} = \int \cos \phi \, d\phi = 2 \cos \phi_{CIJ} \sin \phi_{RI}, \tag{4-30}$$

$$F_{4IJ} = \int \sin\phi \cos\phi \, d\phi = 2 \sin\phi_{CIJ} \cos\phi_{CIJ} \sin\phi_{RI} \cos\phi_{RI}, \tag{4-31}$$

$$F_{5IJ} = \int \cos^2\phi \, d\phi = \phi_{RI} + \sin\phi_{RI} \cos\phi_{RI} (\cos^2\phi_{CIJ} - \sin^2\phi_{CIJ}), \tag{4-32}$$

where all integrations are over the range stated.

The result for the IJ^{th} zone is then

$$\begin{aligned}\overrightarrow{dP}_{AIJ} = \frac{P_S A_E R_E^2}{\pi Q^4} \sin\beta (R_O \cos\beta - R_E) \, d\beta \Big[& \bar{X}_A (R_O - R_E \cos\beta) \\ & (F_{1IJ} S_{XA} \cos\beta + F_{3IJ} S_{YA} \sin\beta) \\ & - \bar{Y}_A R_E \sin\beta (F_{3IJ} S_{XA} \cos\beta + F_{5IJ} S_{YA} \sin\beta) \\ & - \bar{Z}_A R_E \sin\beta (F_{2IJ} S_{XA} \cos\beta + F_{4IJ} S_{YA} \sin\beta) \Big].\end{aligned} \tag{4-33}$$

This expression is of the form

$$\begin{aligned}\overrightarrow{dP}_{AIJ} = & \bar{X}_A (dG_{XXIJ} S_{XA} + dG_{XYIJ} S_{YA}) \\ & + \bar{Y}_A (dG_{YXIJ} S_{XA} + dG_{YYIJ} S_{YA}) \\ & + \bar{Z}_A (dG_{ZXIJ} S_{XA} + dG_{ZYIJ} S_{YA}).\end{aligned} \tag{4-34}$$

Each of the functions G_{--IJ} is determined by numerical integration with respect to β, over the range indicated by Equation 4-17. Each annulus I will give a different result, as well as each azimuthal segment J. This is because of the functions F_{-IJ} in Equation 4-33. (It should be noted that Q is a function of β.)

All of the computations up to and including the computations of the G_{--IJ} should be done by a separate computer program, or in an initialization module of the main program. The resulting $6\ (2\ N_B - 1)^2$ values of the G_{--IJ} are then stored for use in the environmental module of the main program.

At each time interval for which it is desired to compute the albedo forces and torques, the components, S_{XA} and S_{YA}, are computed from Equations 4-4 and 4-5. Each earth zone is then treated as an auxiliary "sun." The multiplication of the G_{--IJ} by S_{XA} and S_{YA} yields the components of

$$\vec{P}_{AIJ} = \vec{X}_A P_{AXIJ} + \vec{Y}_A P_{AYIJ} + \vec{Z}_A P_{AZIJ}. \tag{4-35}$$

The magnitude of the albedo pressure, due to reflection from the IJ^{th} zone, is

$$P_{AIJ} = \sqrt{P_{AXIJ}^2 + P_{AYIJ}^2 + P_{AZIJ}^2}. \tag{4-36}$$

Its direction cosines are

$$A_{AIJ} = \frac{P_{AXIJ}}{P_{AIJ}}, \tag{4-37}$$

$$B_{AIJ} = \frac{P_{AYIJ}}{P_{AIJ}}, \tag{4-38}$$

and

$$C_{ALJ} = \frac{P_{AZLJ}}{P_{ALJ}} \quad . \tag{4-39}$$

The direction cosines in the satellite main reference frame are computed from Equation 4-19. The information that is available for the solar flux is now available for the albedo flux from each zone.

The computation for the albedo forces and torques (due to reflection from each zone) then proceeds in the same manner as for solar effects, as described in Sections 5 and 6. When the effects for every sunlit zone have been computed, they are added vectorially to obtain the total effects.

It is emphasized that the total effects can not be computed from a "resultant" flux which is the vector sum of the zone fluxes. Superposition of fluxes from different directions is not applicable because of the nonlinear nature of the effects, and because of body shadows.

SECTION 5

BODY SHADOWS

The analysis of the effects of shading of one part of the body by another is a simplification of the method described in References 5 and 6. The basic method is flexible enough to accommodate a configuration consisting of any number of flat plates and bodies of revolution. However, practical limitations of computer storage and running time must be considered. The method will be explained as though applied to solar radiation pressure effects, although it is equally applicable to aerodynamic and albedo pressure effects.

The entire satellite surface is subdivided into zones, and a central point is associated with each of these zones. An entire zone is considered sunlit if its central point is sunlit; the entire zone is considered shaded if its central point is shaded. Thus, the shadow analysis treats only the shading of points. The gridding should be sufficiently fine for reasonable accuracy. It should conform to the gridding used for structural dynamical analysis or constitute a further subdivision thereof.

The central point of a zone is tested for shading by every sub-body of the satellite configuration until it is found to be shaded by one of them. At this point, such testing for that central point is terminated. If the central point of a zone is not shaded by any sub-body, that zone is sunlit.

The method will be illustrated by using several simple shapes as examples. Subsequently, the generalization to a general body of revolution will be presented.

5.1 FLAT PLATES

A point A shaded by the I^{th} flat plate is shown in Figure 5-1. In order that the plate shades the point, two conditions are necessary and sufficient. The first is that the line through point A and parallel to the solar unit vector $\bar{S}$ intersects the plane of the plate at some point P which lies within the boundaries of the plate. Secondly, point P must

be "upstream" (i.e., toward the sun) from point A. A sub-body composed of flat plates shades point A if any one or more of the flat plates shades the point. If none of the flat plates shades point A, that body does not shade point A.

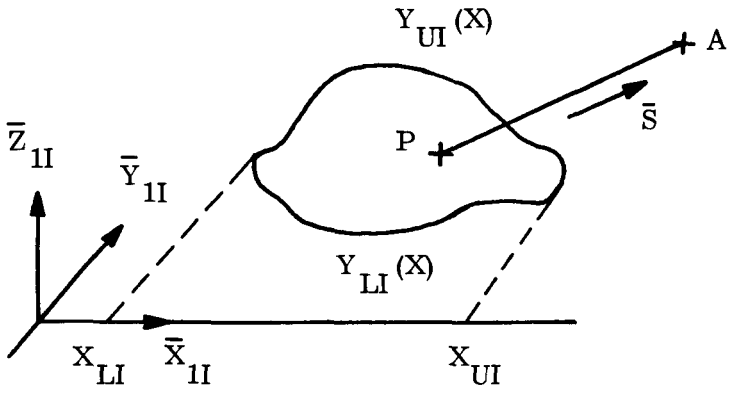

Figure 5-1. Shading by a Flat Plate

The determination of whether a particular flat plate shades a particular point is facilitated by using a reference frame such that the flat plate lies in one of the reference planes. The coordinates of point P in this plane are given by X_P and Y_P. The vector from the origin to point P is

$$\vec{P} = X_{1I} X_P + Y_{1I} Y_P. \tag{5-1}$$

The coordinates of point A are X_A, Y_A, and Z_A. The vector from the origin to point A is

$$\vec{A} = \bar{X}_{1I} X_A + \bar{Y}_{1I} Y_A + \bar{Z}_{1I} Z_A. \tag{5-2}$$

The direction cosines of the solar unit vector $\bar{S}$ in the I^{th} flat plate reference frame are S_{X1I}, S_{Y1I}, and S_{Z1I}. The vector from point P to point A has an unknown magnitude, U. The vector is

$$\vec{PA} = \bar{X}_{1I} S_{X1I} U + \bar{Y}_{1I} S_{Y1I} U + \bar{Z}_{1I} S_{Z1I} U. \tag{5-3}$$

From Figure 5-1,

$$\vec{P} + \vec{PA} = \vec{A}. \tag{5-4}$$

Equation 5-4 is written in terms of its rectangular components,

$$X_P + S_{X1I}\, U = X_A, \tag{5-5}$$

$$Y_P + S_{Y1I}\, U = Y_A, \tag{5-6}$$

$$S_{Z1I}\, U = Z_A. \tag{5-7}$$

This is written in matrix form and solved for the unknowns X_P, Y_P, and U,

$$\begin{bmatrix} X_P \\ Y_P \\ U \end{bmatrix} = \begin{bmatrix} 1 & 0 & S_{X1I} \\ 0 & 1 & S_{Y1I} \\ 0 & 0 & S_{Z1I} \end{bmatrix}^{-1} \begin{bmatrix} X_A \\ Y_A \\ Z_A \end{bmatrix}. \tag{5-8}$$

Since

$$U = \frac{Z_A}{S_{Z1I}} \tag{5-9}$$

a singularity could be encountered. To prevent this, S_{Z1I} should be tested prior to any other computations. If its absolute value is less than a prescribed threshold or tolerance value, no computations should be done. In that case, the point should be considered not to be shaded by the flat plate. Likewise, if Z_A is close to zero, the point should be considered not shaded. The case where both S_{Z1I} and Z_A are close to zero is considered trivial. If neither of these is zero, the solution to Equation 5-8 is given by Equation 5-9 and by

$$X_P = X_A - S_{X1I}\, U, \tag{5-10}$$

$$Y_P = Y_A - S_{Y1I}\, U. \tag{5-11}$$

If a negative value of U is obtained from Equation 5-9, point P is downstream from point A, and point A is not shaded by the I^{th} flat plate. In this case, the subsequent computations for point A and this flat plate are omitted. If U is positive, X_P and Y_P are solved for and the determination made as to whether point P lies within the boundary of the flat plate. If X_P lies outside the range X_{LI}, X_{UI} shown in Figure 5-1, point A is not shaded by the flat plate. If X_P lies within the range, it is necessary to test whether Y_P lies within the range $Y_{LI}(X_P)$, $Y_{UI}(X_P)$, where Y_{LI} and Y_{UI} describe the boundaries of the flat plate as functions of X, as shown in Figure 5-1. If Y_P lies outside the range, point A is not shaded by the flat plate. If Y_P lies inside the range, point A is shaded by the flat plate.

If point A is not shaded by the I^{th} flat plate, testing continues with the other flat plates.

5.2 SPHERES

A point A shaded by the J^{th} sphere is shown in Figure 5-2. The triad representing the reference frame for this sphere is shown at one side for clarity. Actually, the origin of the reference frame is at the center of the sphere.

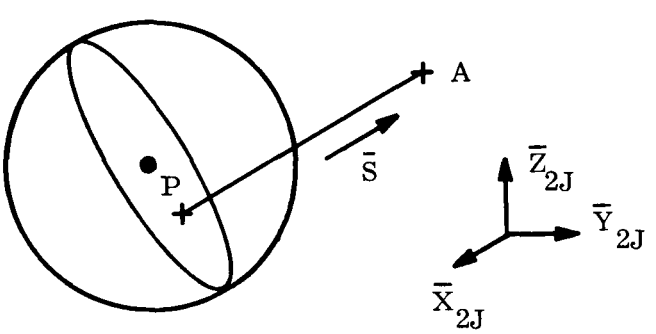

Figure 5-2. Shading by a Sphere

Two conditions are necessary and sufficient for the sphere to shade point A. The first is that the line through point A and parallel to the solar unit vector $\bar{S}$ passes through the sphere. Secondly, the sphere must be "upstream" from the point.

The solar unit vector is expressed in terms of its components in the sphere reference frame,

$$\bar{S} = \bar{X}_{2J} S_{X2J} + \bar{Y}_{2J} S_{Y2J} + \bar{Z}_{2J} S_{Z2J}. \tag{5-12}$$

The equation of the plane passing through the center of the sphere and perpendicular to $\bar{S}$ is

$$S_{X2J} x + S_{Y2J} y + S_{Z2J} z = 0. \tag{5-13}$$

The vector from the origin to point P is

$$\vec{P} = \bar{X}_{2J} X_P + \bar{Y}_{2J} Y_P + \bar{Z}_{2J} Z_P, \tag{5-14}$$

where X_P, Y_P, and Z_P are the coordinates of point P. The vector from the origin to A is

$$\vec{A} = \bar{X}_{2J} X_A + \bar{Y}_{2J} Y_A + \bar{Z}_{2J} Z_A. \tag{5-15}$$

The vector from point P to point A has the unknown magnitude U,

$$\vec{PA} = \bar{X}_{2J} S_{X2J} U + \bar{Y}_{2J} S_{Y2J} U + \bar{Z}_{2J} S_{Z2J} U. \tag{5-16}$$

From Figure 5-2,

$$\vec{P} + \vec{PA} = \vec{A}. \tag{5-17}$$

This equation is written in terms of its rectangular components,

$$X_P + S_{X2J}\, U = X_A, \tag{5-18}$$

$$Y_P + S_{Y2J}\, U = Y_A, \tag{5-19}$$

$$Z_P + S_{Z2J}\, U = Z_A. \tag{5-20}$$

Because $\vec{P}$ is perpendicular to $\vec{PA}$, their dot product is zero,

$$X_P S_{X2J} + Y_P S_{Y2J} + Z_P S_{Z2J} = 0. \tag{5-21}$$

The last four equations constitute a set of simultaneous equations with four unknowns. The solution is

$$U = X_A S_{X2J} + Y_A S_{Y2J} + Z_A S_{Z2J}, \tag{5-22}$$

$$X_P = X_A - U S_{X2J}, \tag{5-23}$$

$$Y_P = Y_A - U S_{Y2J}, \tag{5-24}$$

$$Z_P = Z_A - U S_{Z2J}. \tag{5-25}$$

If a negative value of U is obtained, point P is downstream from point A; and point A is not shaded by the J^{th} sphere. In this case, the subsequent computations for point A and this sphere are omitted.

If

$$X_P^2 + Y_P^2 + Z_P^2 \tag{5-26}$$

is greater than the square of the radius of the sphere, the point A is not shaded by the sphere. Otherwise, it is shaded.

In lieu of the expression 5-26, the equivalent expression,

$$X_A^2 + Y_A^2 + Z_A^2 - U^2, \qquad (5\text{-}26a)$$

may be used. This leads to a shorter computation, since Equations 5-23, 5-24, and 5-25 may be omitted.

If the point A is not shaded by the J^{th} sphere, testing continues with the other spheres.

5.3 CYLINDERS

A point A shaded by the K^{th} cylinder is shown in Figure 5-3. Another view, with the solar unit vector $\bar{S}$ in the plane of the figure, is shown in Figure 5-4. Here, the cylinder is represented by its two end circles and a rectangle, all shown on edge. The plane of the rectangle contains the axis of the cylinder and makes the maximum possible angle with the sun. The rectangle, which is bounded by the cylinder, is designated as the shadow rectangle; and the end circles are designated as shadow circles. These names arise from the two necessary and sufficient conditions for shading of point A by the cylinder.

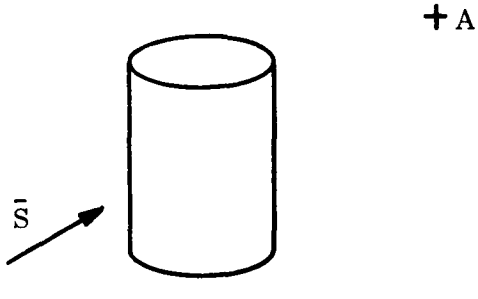

Figure 5-3. Shading by a Cylinder

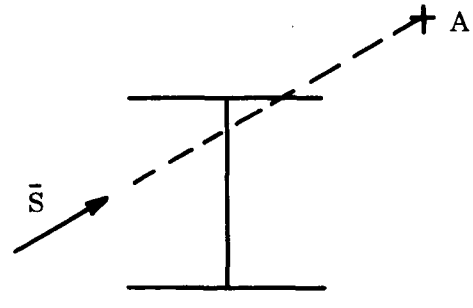

Figure 5-4. The Shadow Rectangle and Circles

The first is that the line through point A and parallel to the solar unit vector $\bar{S}$ must pass through one or more of the plane surfaces, designated as shadow rectangle and shadow circles. The second condition is that the cylinder must be "upstream" from the point.

The shadow circles are tested first. Point A, shaded by a shadow circle, is shown in Figure 5-5. The origin of the cylinder reference frame is at the geometric center of the cylinder, and the center of the circle is distant X_P from this origin. Then, the vector from the origin to point P is

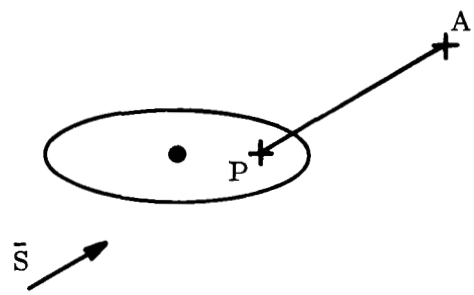

Figure 5-5. Shading by a Circular Surface

$$\vec{P} = \bar{X}_{3K} X_P + \bar{Y}_{3K} Y_P + \bar{Z}_{3K} Z_P. \qquad (5\text{-}27)$$

The solar unit vector $\bar{S}$ is expressed in the reference frame of the K^{th} cylinder,

$$\bar{S} = \bar{X}_{3K} S_{X3K} + \bar{Y}_{3K} S_{Y3K} + \bar{Z}_{3K} S_{Z3K}. \qquad (5\text{-}28)$$

The vector from the origin to point A is

$$\vec{A} = \bar{X}_{3K} X_A + \bar{Y}_{3K} Y_A + \bar{Z}_{3K} Z_A. \qquad (5\text{-}29)$$

The vector from point P to point A is of unknown magnitude U,

$$\vec{PA} = \bar{X}_{3K} S_{X3K} U + \bar{Y}_{3K} S_{Y3K} U + \bar{Z}_{3K} S_{Z3K} U. \qquad (5\text{-}30)$$

From Figure 5-5,

$$\vec{P} + \vec{PA} = \vec{A}. \tag{5-31}$$

Equation 5-31 is written in terms of its rectangular components,

$$X_P + S_{X3K} U = X_A, \tag{5-32}$$

$$Y_P + S_{Y3K} U = Y_A, \tag{5-33}$$

$$Z_P + S_{Z3K} U = Z_A. \tag{5-34}$$

These constitute three simultaneous equations in the three unknowns, U, Y_P, and Z_P. Because X_P is known, Equation 5-32 is first solved for U,

$$U = \frac{X_A - X_P}{S_{X3K}} \tag{5-35}$$

Then,

$$Y_P = Y_A - S_{Y3K}U, \tag{5-36}$$

$$Z_P = Z_A - S_{Z3K}U. \tag{5-37}$$

If

$$Y_P^2 + Z_P^2 \tag{5-38}$$

is greater than the square of the radius of the cylinder, point A is not shaded by the circular surface. Otherwise, it is so shaded.

If S_{X3K} is nearly zero, Equation 5-35 has a singularity. In such a case, the solar rays are nearly perpendicular to the axis of the K^{th} cylinder. In this case, the circular end can not shade point A.

The test for the singularity should be done first. Then, if the singular case is not found, the general equations are used.

The other flat circular end of the K^{th} cylinder is tested in the same manner. The only difference is that the X_P coordinate has a different numerical value for each circular end. If the singular case occurs with the first circular end, the other need not be tested. In the singular case, neither circular end can shade point A.

The shadow rectangle of the K^{th} cylinder is tested next. A point A shaded by this rectangle is shown in Figure 5-6. The center of the rectangle is the origin of the reference frame of the K^{th} cylinder. It is convenient to use a shadow reference frame, one of whose planes contains the shadow rectangle. This reference frame is defined by the $\bar{X}_{3K}$ $\bar{Y}_R$ $\bar{Z}_R$ orthonormal triad, and is obtained from the reference frame of the K^{th} cylinder by a rotation about the $\bar{X}_{3K}$ axis through an angle such that the solar unit vector $\bar{S}$ has a positive $\bar{Y}_R$ component and no $\bar{Z}_R$ component. The transformation is

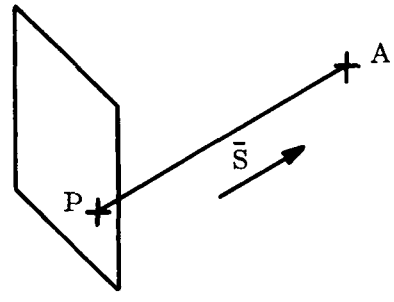

Figure 5-6. Shading by the K^{th} Shadow Rectangle

$$\begin{bmatrix} \bar{Y}_R \\ \\ \bar{Z}_R \end{bmatrix} = \frac{1}{\sqrt{S_{Y3K}^2 + S_{Z3K}^2}} \begin{bmatrix} S_{Y3K} & S_{Z3K} \\ \\ -S_{Z3K} & S_{Y3K} \end{bmatrix} \begin{bmatrix} \bar{Y}_{3K} \\ \\ \bar{Z}_{3K} \end{bmatrix} \tag{5-39}$$

Equations 5-27 through 5-37 hold, but the rectangular components in the shadow reference frame are used. The counterparts of Equations 5-32 through 5-34 are

$$X_P + S_{X3K} U = X_A , \tag{5-40}$$

$$U = \frac{S_{Y3K} Y_A + S_{Z3K} Z_A}{S_{Y3K}^2 + S_{Z3K}^2} , \tag{5-41}$$

$$Z_Q = \frac{S_{Y3K} Z_A - S_{Z3K} Y_A}{\sqrt{S_{Y3K}^2 + S_{Z3K}^2}} . \tag{5-42}$$

U is first computed from Equation 5-41. If it is negative, the shadow rectangle is downstream from point A, and therefore does not shade point A. If U is positive, X_P is computed from the solution of Equation 5-40,

$$X_P = X_A - S_{X3K} U. \tag{5-43}$$

The absolute value of X_P is compared with the half-length of the cylinder. If the former is greater, point P lies outside the rectangle, and therefore does not shade point A. Otherwise, Z_Q is computed from Equation 5-42. This is the transverse coordinate of point P in the

shadow reference frame. If the absolute value of Z_Q is greater than the radius of the cylinder, the rectangle does not shade point A. Otherwise, it does.

If

$$S_{Y3K}^2 + S_{Z3K}^2 \tag{5-44}$$

is nearly zero a singularity is encountered.

This expression should be tested first. If the singularity occurs, the solar rays are nearly parallel to the cylinder axis, and the rectangle does not shade point A.

5.4 CONES AND CONE FRUSTUMS

Although there are many points of similarity, a cone can not be treated as a cylinder of varying radius. This is because the shadow lines on the surface of the cone do not, in general, define a plane which contains the axis of the cone. However, the shadow lines, which are the boundaries between the shaded and sunlit portions of the surface, are the key to the analysis.

It is convenient to define a shadow reference frame for the cone in the same manner as was done for the cylinder. This frame is defined by the $\bar{X}_R$ $\bar{Y}_R$ $\bar{Z}_R$ triad of orthonormal vectors, with the origin at the apex of the cone (extended from the frustum if necessary). The $\bar{X}_R$ axis is positive in the direction from the apex outward along the cone. The $\bar{X}_R$ $\bar{Z}_R$ plane contains the axis of the cone, and makes the maximum possible angle with the solar unit vector. The transformation from the cone reference frame to its shadow reference frame is given by Equation 5-39, although different subscripts would be used for the original cone reference frame.

The equation of the cone is

$$y^2 + z^2 = b^2 x^2 , \tag{5-45}$$

where b is the tangent of the half-angle at the apex. The unit vector normal to the surface of the cone at any point is

$$\bar{N} = \frac{-\bar{X}_R b^2 x + \bar{Y}_R y + \bar{Z}_R z}{b \times \sqrt{b^2 + 1}}. \tag{5-46}$$

The solar unit vector is

$$\bar{S} = \bar{X}_R S_{XR} + \bar{Y}_R S_{YR}. \tag{5-47}$$

Along the shadow line on the surface of the cone, $\bar{N}$ and $\bar{S}$ are perpendicular, so their dot product is zero. This leads to an equation for Y_S, the value of y on the shadow line,

$$Y_S = \frac{S_{XR}}{S_{YR}} b^2 x. \tag{5-48}$$

From Equation 5-45, the corresponding value of z is

$$Z_S = \pm \frac{bx}{S_{YR}} \sqrt{S_{YR}^2 - b^2 S_{XR}^2}. \tag{5-49}$$

These equations define two straight lines which are the boundaries of the shadow triangle of the cone, or of the shadow trapezoid of the cone frustum. The shadow triangle or trapezoid plays the same role as the shadow rectangle of the cylinder.

The end circle of the cone, or the two end circles of the cone frustum, are treated in the same manner as those of the cylinder.

The form of Equation 5-49 indicates that several cases must be distinguished.

First, if the solar rays make a sufficiently small angle with the cone axis, such that

$$\frac{S_{YR}}{S_{XR}} \leqq b, \tag{5-50}$$

the entire conical surface is sunlit, and only the end circle(s) need be tested. Equations 5-35 through 5-38 are used for this purpose, with appropriate changes in the subscripts.

Secondly, if

$$\left| \frac{S_{YR}}{S_{XR}} \right| > b, \tag{5-51}$$

the solar rays make a sufficiently large angle with the cone axis such that the conical surface is only partly sunlit. This is the general case. A point A shaded by the shadow triangle is shown in Figure 5-7. The coordinates of point P, which casts the shadow in the shadow reference frame, are X_P, Y_P, and Z_P. The vector from the origin at the apex, to point P is

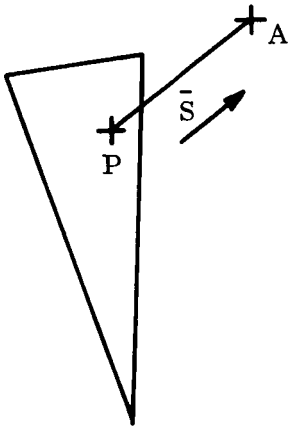

Figure 5-7. Shading by a Cone

$$\vec{P} = \bar{X}_R X_P + \bar{Y}_R Y_P + \bar{Z}_R Z_P. \tag{5-52}$$

Since point P is in the plane of the shadow triangle,

$$Y_P = Y_S (X_P) = \frac{S_{XR}}{S_{YR}} b^2 X_P. \tag{5-53}$$

The vector from point P to point A is of unknown magnitude U,

$$\overrightarrow{PA} = \bar{X}_R S_{XR} U + \bar{Y}_R S_{YR} U. \tag{5-54}$$

The coordinates of point A in the shadow reference frame are X_A, Y_A, and Z_A. The vector from the origin to point A is

$$\vec{A} = \bar{X}_R X_A + \bar{Y}_R Y_A + \bar{Z}_R Z_A. \tag{5-55}$$

Equation 5-31 holds. This is rewritten in terms of its rectangular components,

$$X_P + S_{XR} U = X_A, \tag{5-56}$$

$$Y_P + S_{YR} U = Y_A, \tag{5-57}$$

$$Z_P = Z_A. \tag{5-58}$$

Equation 5-58 is explicitly solved for Z_P. Equations 5-53, 5-56, and 5-57 are three simultaneous linear equations with the three unknowns, X_P, Y_P, and U.

Their solution is

$$X_P = \frac{S_{YR} (S_{YR} X_A - S_{XR} Y_A)}{S_{YR}^2 - b^2 S_{XR}^2}, \tag{5-59}$$

$$Y_P = \frac{b^2 S_{XR} (S_{YR} X_A - S_{XR} Y_A)}{S_{YR}^2 - b^2 S_{XR}^2}, \tag{5-60}$$

$$U = \frac{S_{YR}\, Y_A - b^2 S_{XR}\, X_A}{S_{YR}^{\,2} - b^2 S_{XR}^{\,2}} \tag{5-61}$$

The value X_P is used for x in Equation 5-49. Equation 5-49 is then solved for Z_S. If $|Z_A|$ is equal to or less than $|Z_S|$, point A is shaded by the conical surface. Otherwise, it is not shaded.

The third case is that for which

$$\frac{S_{YR}}{S_{XR}} \leqq -b. \tag{5-62}$$

Then, the entire conical surface is shaded, and only the end circle(s) need be tested.

5.5 GENERAL BODIES OF REVOLUTION

The general body of revolution may be considered as a sequence of coaxial cone frustums, of vanishingly small lengths. A shadow reference frame is defined in the same manner as for the cylinder and the cone. Equations 5-47, 5-52, and 5-54 through 5-58 hold.

If the profile of the surface is represented in any plane through the axis of symmetry by

$$r = f(x), \tag{5-63}$$

where r is the radius at any point along the axis, then the equation of the surface is

$$y^2 + z^2 = [\, f(x) \,]^2 \tag{5-64}$$

The unit vector normal to the surface at any point is

$$\bar{N} = \frac{-\bar{X}_R \, f\, g + \bar{Y}_R \, y + \bar{Z}_R \, z}{f \sqrt{1 + g^2}}, \tag{5-65}$$

where f stands for f (x), and

$$g \equiv \frac{df}{dx} . \tag{5-66}$$

On the shadow line, the dot product of $\bar{S}$ and $\bar{N}$ is zero. This yields

$$Y_S = \frac{S_{XR}}{S_{YR}} \, f\, g, \tag{5-67}$$

$$Z_S = \pm \frac{f}{S_{YR}} \sqrt{S_{YR}^2 - g^2 S_{XR}^2} . \tag{5-68}$$

Because Y_P is on the shadow surface,

$$Y_P = Y_S (X_P) = \frac{S_{XR}}{S_{YR}} \, f (X_P)\, g (X_P). \tag{5-69}$$

If U is eliminated from Equations 5-56 and 5-57, the result is a linear relation between X_P and Y_P,

$$S_{YR} X_P - S_{XR} Y_P = S_{YR} X_A - S_{XR} Y_A. \tag{5-70}$$

This is combined with Equation 5-69, to eliminate Y_P,

$$S_{YR}^2 X_P - S_{XR}^2 f(X_P)\, g(X_P) = S_{YR}(S_{YR} X_A - S_{XR} Y_A). \tag{5-71}$$

This equation involves only X_P, for which it is solved. The solution is used in Equation 5-68 to find Z_S. Then $|Z_A|$ is compared to $|Z_S|$ as in the case of the cone, and the same conclusion applies.

Different cases, which are similar to those of the cone, must be distinguished. If

$$S_{YR} > |S_{XR}\, g(X_P)|, \tag{5-72}$$

the general case exists, and the foregoing equations are valid. If

$$S_{YR} \leqq |S_{XR}\, g(X_P)|,$$

the conical surface is either entirely sunlit or entirely shaded. Then only the end circle(s) need be tested.

In any case, the end circle(s) are tested in the same manner as for the cylinder.

SECTION 6
FORCES AND TORQUES

The forces and torques on bodies of various shapes are developed in terms of solar radiation pressure. The equations so derived are easily extended to aerodynamic and albedo pressure by simple analogies which are described.

The basic equation for solar radiation pressure effects is the equation for the element of solar force, d^2F_S, on an element of body surface area, dA.

$$d^2F_S = P_S dA \left[\bar{S} (\bar{S} \cdot \bar{N}) (1 - \rho_S) + 2\bar{N}\rho_S (\bar{S} \cdot \bar{N})^2 + \frac{2}{3} \bar{N}\rho_D (\bar{S} \cdot \bar{N}) \right]. \qquad (6\text{-}1)$$

Here, P_S is the solar pressure, $\bar{S}$ is a unit vector in the direction of the solar flux at the satellite, $\bar{N}$ is the unit vector normal to dA and positive inward, ρ_S is the specular reflectance of the surface, and ρ_D is the diffuse reflectance of the surface. This equation is derived in Section 11 of Reference 3, and the major assumptions used are stated there.

The basic equation for aerodynamic pressure effects at high altitudes is also the element of force on an element of area.

$$d^2F_A = P_A d_A (\bar{V} \cdot \bar{N}) (\bar{V} + \frac{2}{3} \bar{N}C_V) \qquad (6\text{-}2)$$

P_A is the aerodynamic pressure, $\bar{V}$ is a unit vector in the direction of the relative wind, and C_V is the ratio of particle reflected velocity to particle incident velocity. This equation is derived in Section 17 of Reference 3, and the major assumptions are stated there.

Equation 6-2 is exactly analogous to Equation 6-1, if P_A is substituted for P_S, $\bar{V}$ is substituted for $\bar{S}$, ρ_S is set equal to zero, and C_V is substituted for ρ_D.

The effect of the albedo flux from each individual earth zone is like the effect of the solar flux, to the extent that the approximation of the zone as a point source is a good one. The basic equation for the albedo force, due to the reflection from a single earth zone, is similar to Equation 6-1. However, the magnitude of the pressure is different, and the unit vector in the direction of the albedo flux must be substituted for $\bar{S}$.

The magnitude and direction of the albedo flux are derived in Section 4.

The solar force on a flat plate is given by Equation 6-1, with the entire area A substituted for the element of area, dA. Although the force is actually distributed over the surface as a uniform pressure, for the purpose of computing the solar torque, the force is considered to be applied to the centroid of the area. The torque is usually computed about axes through a specified reference point. For the flat plate, the torque is the vector crossproduct of the moment arm from the reference point to the centroid of the plate and the force.

Any body may be approximated as a combination of flat plates. Such a representation is especially advantageous in cases where the shadow geometry is complicated or where structural flexibility produces appreciable distortion.

It is not desirable to limit the analysis to flat plates and aggregations of flat plates. This is because situations will arise where a large rigid body is not shaded except by itself; and if it is a body of revolution, advantage of the consequent symmetry may be taken.

The solar torque on a sphere, not shaded by another body, is

$$\vec{T}_{SS} = \pi P_S A_S^2 \left(1 + \frac{4}{9} \rho_D\right) (\vec{R}_S \times \bar{S}). \qquad (6\text{-}3)$$

where A_S is the radius of the sphere, and $\vec{R}_S$ is the vector from the reference point to the center of the sphere.

The equations for the solar force and torque on a cylinder have two uses. The first, already mentioned, is the case of a rigid cylinder not shaded by another body. The second is the case of a long thin rod or tube, such as a gravity radient rod, an instrument boom, or a connecting member of a large composite structure, where the following especially simple shadow analysis yields a good approximation. If the length is much greater than the diameter, the former may be subdivided into sufficiently short segments so that each one may be considered entirely sunlit or entirely shaded. Then the shadow analysis of each segment may be simplified by considering a single reference or central point in that segment. This is simpler than dividing the periphery of the segment to obtain a number of zones to be approximated as flat plates.

The solar forces and torques on a cylinder are most conveniently expressed in a reference frame one of whose planes contains the sun. The shadow reference frame previously described is suitable and convenient. The $\bar{X}_R$ component of the solar force on the cylindrical surface is

$$F_{SXR} = 2P_S R_C L_C S_{XR} S_{YR} (1 - \rho_S), \tag{6-4}$$

where R_C is the radius, and L_C the length of the cylinder. The $\bar{Y}_R$ component is

$$F_{SYR} = 2 P_S R_C L_C S_{YR} \left[S_{YR} (1 + \frac{1}{3} \rho_S) + \frac{\pi}{6} \rho_D \right] \tag{6-5}$$

The $\bar{Z}_R$ component is zero.

For the purpose of torque computations, the vector from any reference point to the geometric center of the cylinder is expressed as

$$\vec{R}_G = \bar{X}_R X_G + \bar{Y}_R Y_G + \bar{Z}_R Z_G \tag{6-6}$$

Then the vector from the reference point to any surface element is

$$\vec{R} = \vec{R}_G - \bar{N} R_C + \bar{X}_R x, \tag{6-7}$$

where x is the length coordinate.

The torque about axes passing through the reference point is the vector crossproduct of this vector and the force. The $\bar{X}_R$ component of the torque is

$$T_{SXR} = -Z_G F_{SYR} . \tag{6-8}$$

The $\bar{Y}_R$ component is

$$T_{SYR} = Z_G F_{SXR} . \tag{6-9}$$

The $\bar{Z}_R$ component is

$$T_{SZR} = X_G F_{SYR} - Y_G F_{SXR} + \frac{\pi}{2} P_S R_C^2 L_C S_{XR} S_{YR} (1 - \rho_S) \tag{6-10}$$

For long thin rods or tubes, the contribution of the radius to the moment arm may be neglected, by deleting the last term of the last equation.

If the cylindrical surface is not uniform, the foregoing equations are not valid for the cylinder as a whole. If the surface is subdivided into cylindrical "bands," each of which has uniform characteristics, each band is considered as a cylinder, and the foregoing equations are applied to each one separately. If the surface is subdivided in any other manner, it is simplest to form a grid of zones sufficiently small to be treated as flat plates.

In any case, the flat ends of a cylinder, if sunlit, are treated as flat plates.

The solar forces and torques on a cone are calculated by using the same reference frame as for the shadow analysis and also a cylindrical coordinate frame. The apex of the cone is the origin of both frames. The cylindrical angular coordinate is ψ, and the radial coordinate is r. ψ is zero along the line of symmetry of the sunlit portion of the surface.

Then

$$r^2 = y^2 + z^2 \tag{6-11}$$

$$r = bx \tag{6-12}$$

$$y = -r \cos \psi \tag{6-13}$$

$$z = r \sin \psi \tag{6-14}$$

$$\tan \psi = -\frac{z}{y}. \tag{6-15}$$

The unit normal vector, positive inward toward the sunlit surface, is

$$\bar{N} = \frac{\bar{X}_R b + \bar{Y}_R \cos \psi + \bar{Z}_R \sin \psi}{\sqrt{b^2 + 1}} \tag{6-16}$$

The solar unit vector $\bar{S}$ is given by Equation 5-47, and

$$\bar{S} \cdot \bar{N} = \frac{bS_{XR} + S_{YR} \cos \psi}{\sqrt{b^2 + 1}} \tag{6-17}$$

The element of area on the conical surface is

$$dA = b\,x\,\sqrt{b^2+1}\;\;dx\,d\psi \tag{6-18}$$

The components of the element of force on dA, in the shadow reference frame, are

$$d^2F_{SXR} = P_S\,bx\,dx\,d\psi\left\{(bS_{XR}+S_{YR}\cos\psi)\left[S_{XR}(1-\rho_S)+\frac{\frac{2}{3}\rho_D b}{\sqrt{b^2+1}}\right]+\frac{2\rho_S b}{b^2+1}(bS_{XR}+S_{YR}\cos\psi)^2\right\} \tag{6-19}$$

$$d^2F_{SYR} = P_S\,bx\,dx\,d\psi\left\{(bS_{XR}+S_{YR}\cos\psi)\left[S_{YR}(1-\rho_S)+\frac{\frac{2}{3}\rho_D\cos\psi}{\sqrt{b^2+1}}\right]+\frac{2\rho_S\cos\psi}{b^2+1}(bS_{XR}+S_{YR}\cos\psi)^2\right\} \tag{6-20}$$

$$d^2F_{SZR} = P_S\,bx\sin\psi\,dx\,d\psi\left[\frac{\frac{2}{3}\rho_D}{\sqrt{b^2+1}}(bS_{XR}+S_{YR}\cos\psi)+\frac{2\rho_S}{b^2+1}(bS_{XR}+S_{YR}\cos\psi)^2\right] \tag{6-21}$$

The same cases used previously are defined here. The first case is defined by Equation 5-50. The whole conical surface is sunlit, and the solar forces are computed by integrating the above equations with respect to ψ between the limits of $-\pi$ and $+\pi$, and with respect to x between the

limits of X_L and X_U. These values of x correspond to the ends of the cone frustum. For a cone, X_L is zero. The results of the integration are the components of the solar force in the shadow reference frame.

$$F_{SXR} = \pi P_S b^2 (X_U^2 - X_L^2) \left[S_{XR}^2 (1 + \rho_S) + \frac{\frac{2}{3} \rho_D b S_{XR}}{\sqrt{b^2 + 1}} \right.$$

$$\left. + \frac{\rho_S}{b^2 + 1} (S_{YR}^2 - 2 S_{XR}^2) \right], \quad (6\text{-}22)$$

$$F_{SYR} = \pi P_S b S_{YR} (X_U^2 - X_L^2) \left[b S_{XR} \left(1 - \rho_S + \frac{2 \rho_S}{b^2 + 1} \right) + \frac{\rho_D}{3\sqrt{b^2 + 1}} \right], \quad (6\text{-}23)$$

$$F_{SZR} = 0. \quad (6\text{-}24)$$

For computing solar torques, the vector from a specified reference point to the apex of the cone is designated

$$\vec{R}_G = \bar{X}_R X_G + \bar{Y}_R Y_G + \bar{Z}_R Z_G. \quad (6\text{-}25)$$

Then the vector from the reference point to the element of area, dA, is

$$\vec{R} = \bar{X}_R (X_G + x) + \bar{Y}_R (Y_G - b x \cos \psi) + \bar{Z}_R (Z_G - bx \sin \psi). \quad (6\text{-}26)$$

The solar torque, about axes passing through the reference point, is the vector crossproduct of $\vec{R}$ and the solar force. The integration is performed in the same manner as for the force components. This yields the torque components,

$$T_{SXR} = -Z_G F_{SYR}, \tag{6-27}$$

$$T_{SYR} = Z_G F_{SXR}, \tag{6-28}$$

$$T_{SZR} = X_G F_{SYR} - Y_G F_{SXR} + \frac{2}{3} \pi P_S b S_{YR} \left(X_U^3 - X_L^3 \right)$$

$$\cdot \left[\frac{\rho_D}{\sqrt{b^2 + 1}} + 2b S_{XR} \left(1 + \frac{\rho_S b^2}{b^2 + 1} \right) \right] . \tag{6-29}$$

The second case is defined by Equation 5-51. In this case, the conical surface is only partly sunlit. On the shadow line, $\bar{S}$ and $\bar{N}$ are perpendicular. Setting the right hand member of Equation 6-17 equal to zero yields an equation for ψ_S, the value of ψ on the shadow line.

$$\cos \psi_S = - \frac{b S_{XR}}{S_{YR}} , \tag{6-30}$$

$$\sin \psi_S = \sqrt{1 - \frac{b^2 S_{XR}^2}{S_{YR}^2}} , \tag{6-31}$$

$$\psi_S = \mathrm{Cos}^{-1} \left(- \frac{b S_{XR}}{S_{YR}} \right) . \tag{6-32}$$

The solar forces are computed by integrating Equations 6-19 through 6-21 with respect to ψ between the limits of zero and ψ_S, multiplying by two, and integrating with respect to x between the limits of X_L and X_U. The results are the components of the solar force in the shadow reference frame.

$$F_{SXR} = P_S b\left(X_U^2 - X_L^2\right)\left\{(b\,S_{XR}\,\psi_S + S_{YR}\sin\psi_S)\left[S_{XR}\left(1-\rho_S\right)+\frac{\frac{2}{3}\rho_D b}{\sqrt{b^2+1}}\right]\right.$$

$$\left. + \frac{\rho_S b}{b^2+1}\left[\psi_S\left(2b^2 S_{XR}^2 + S_{YR}^2\right) + 3b\,S_{XR}\,S_{YR}\sin\psi_S\right]\right\}, \qquad (6\text{-}33)$$

$$F_{SYR} = P_S b\left(X_U^2 - X_L^2\right)\left\{S_{YR}\,(1-\rho_S)\,(b\,S_{XR}\,\psi_S + S_{YR}\sin\psi_S)\right.$$

$$+ \frac{\frac{1}{3}\rho_D}{\sqrt{b^2+1}}\,(b\,S_{XR}\sin\psi_S + S_{YR}\,\psi_S)$$

$$\left. + \frac{2\rho_S}{b^2+1}\left[b\,S_{YR}\,\psi_S + \frac{1}{3}\sin\psi_S\left(2S_{YR}^2 + b^2 S_{XR}^2\right)\right]\right\}, \qquad (6\text{-}34)$$

$$F_{SZR} = 0. \qquad (6\text{-}35)$$

The solar torques are computed in the same manner as for Case I. Equations 6-25 through 6-28 hold for Case II, also. The $\bar{Z}_R$ component of the torque is

$$T_{SZR} = X_G F_{SYR} - Y_G F_{SXR} + \frac{2}{3} P_S b\left(X_U^3 - X_L^3\right)\left\{\frac{1}{3}\rho_D\sqrt{b^2+1}\,(S_{YR}\,\psi_S\right.$$

$$+ b\,S_{XR}\sin\psi_S) + \frac{1}{2}\,(1+\tfrac{1}{3}\rho_S)\left[3b\,S_{XR}\,S_{YR}\,\psi_S\right.$$

$$\left.\left. + \sin\psi_S\left(2S_{YR}^2 + b^2 S_{XR}^2\right)\right]\right\}. \qquad (6\text{-}36)$$

If

$$\frac{S_{YR}}{S_{XR}} \geqq -b, \tag{6-37}$$

the conical surface is entirely shaded. This is Case III, for which the solar forces and torques on the conical surface are zero.

In any case, the flat end of the cone, or the two ends of the cone frustum, are treated as flat plates if they are sunlit.

The solar forces and torques on a general body of revolution are computed by considering the body as a sequence of coaxial cone frustums of vanishingly small lengths. The profile is again represented by Equation 5-63. Equations 5-64 and 5-66 hold, as well as Equations 6-11 through 6-21, with g substituted for b where it occurs without x, and with f substituted for bx.

If

$$\frac{S_{YR}}{S_{XR}} \leqq g, \tag{6-38}$$

for any range of values of x, then Case I exists throughout that range. The integration of Equations 6-19 through 6-21 with respect to ψ yields,

$$d F_{SXR} = 2\pi P_S f g \, dx \left[S_{XR}^{\,2} (1 + \rho_S) + \frac{2}{3} \rho_D S_{XR} \frac{g}{\sqrt{g^2 + 1}} \right.$$

$$\left. + \frac{\rho_S}{g^2 + 1} \left(S_{YR}^{\,2} - 2 S_{XR}^{\,2} \right) \right], \tag{6-39}$$

$$dF_{SYR} = 2\pi P_S S_{YR} f\,dx \left[g S_{XR} (1 - \rho_S) + \frac{\rho_D}{3\sqrt{g^2 + 1}} + \frac{2\rho_S S_{XR} g}{g^2 + 1} \right] . \quad (6\text{-}40)$$

$$dF_{SZR} = 0 \quad (6\text{-}41)$$

These expressions are integrated with respect to x throughout the range for which condition 6-38 holds. Over this same range, Equations 6-25 through 6-28 hold. The $\overline{Z}_R$ component of the torque is

$$X_G F_{SYR} - Y_G F_{SXR} \quad (6\text{-}42)$$

plus the integral of

$$dT'_{SZR} = x\,dF_{SYR} + \pi P_S S_{YR} f^2 dx \left[\frac{2\rho_D g}{3\sqrt{g^2 + 1}} + S_{XR}\left(1 + 3\rho_S - \frac{4\rho_S}{g^2 + 1}\right)\right], \quad (6\text{-}43)$$

with respect to x.

If

$$\left| \frac{S_{YR}}{S_{XR}} \right| > g, \quad (6\text{-}44)$$

for any range of values of x, then Case II exists throughout that range. Equations 6-30 through 6-32 hold, with g substituted for b. The integration of Equations 6-19 through 6-21 with respect to ψ and multiplication by two yields

$$dF_{SXR} = 2P_S f\,dx \left\{ (g S_{XR} \psi_S + S_{YR} \sin\psi_S) \left[S_{XR}(1-\rho_S) + \frac{2\rho_D g}{3\sqrt{g^2+1}} \right] \right.$$

$$+ \frac{\rho_S g}{g^2+1} \left[\psi_S \left(2g^2 S_{XR}^2 + S_{YR}^2 \right) \right.$$

$$\left. \left. + 3g S_{XR} S_{YR} \sin\psi_S \right] \right\}, \qquad (6\text{-}45)$$

$$dF_{SYR} = 2P_S f\,dx \left\{ S_{YR}(1-\rho_S)(g S_{XR} \psi_S + S_{YR} \sin\psi_S) \right.$$

$$+ \frac{\rho_D}{3\sqrt{g^2+1}} (S_{YR} \psi_S + g S_{XR} \sin\psi_S)$$

$$\left. + \frac{2\rho_S}{g^2+1} \left[g S_{XR} S_{YR} \psi_S + \frac{1}{3} \left(2S_{YR}^2 + g^2 S_{XR}^2 \right) \right] \right\}, \qquad (6\text{-}46)$$

$$dF_{SZR} = 0. \qquad (6\text{-}47)$$

The expressions are integrated with respect to x throughout the range for which Condition 6-44 holds. Over this same range, Equations 6-25 through 6-28 hold, with f substituted for bx in Equation 6-26. The $\bar{Z}_R$ component of the torque is

$$X_G F_{SYR} - Y_G F_{SXR} \qquad (6\text{-}48)$$

plus the integral of

$$d T'_{SZR} = x\, d F_{SYR} + P_S f^2\, dx \left\{ (S_{YR}\, \psi_S + g\, S_{XR} \sin \psi_S) \left[S_{XR} (1 - \rho_S) + \frac{2 \rho_D g}{3\sqrt{g^2 + 1}} \right] + \frac{4 \rho_S g}{g^2 + 1} \left[g\, S_{XR}\, S_{YR}\, \psi_S + \frac{1}{3} \sin \psi_S \left(2 S_{YR}^2 + g^2 S_{XR}^2 \right) \right] \right\}, \quad (6\text{-}49)$$

with respect to x.

If

$$\frac{S_{YR}}{S_{XR}} \geqq -g, \quad (6\text{-}50)$$

for any range of values of x, the surface is entirely shaded throughout that range, and the solar forces and torques are zero.

In any case, the flat ends are treated as flat plates if they are sunlit.

SECTION 7
REFERENCES

1. Hinrichs, R. H., "Attitude Equations for the Applications Technology Satellite," GE Spacecraft Department Document No. 66SD4214, 1 June 1966.

2. Jacchia, L. G., "A Variable Atmospheric Density Model from Satellite Accelerations," Journal of Geophysical Research, V 65 (1960), page 2775.

3. Hinrichs, R. H., "Attitude Dynamics of an N-Rod Satellite," GE Spacecraft Department Document No. 64SD5276, 22 February 1965.

4. Dennison, A. J., "The Illumination of a Cell Surface in Space Due to the Sunlight Reflected from the Earth," GE Missile and Space Vehicle Department Report No. 61SD101, 20 June 1961.

5. Brong, E. A., and S. Matlin, "A Program for the Computation of Newtonian and Free Molecule Forces and Moments for Arbitrary Bodies," GE Re-entry Systems Department Report No. 63SD210, 16 January 1963.

6. Gilman, H. D., "Computation of Forces and Moments on Arbitrary Shaped Bodies-Part I: Analysis and Program Design," GE Re-entry Systems Department Report No. 64SD209, February 1964.

DISTRIBUTION LIST

M. Salyers	U4451
P. Usavage	U4632
O. B. Gates	U2612
F. E. Xydis	U2704
R. E. Roach 10	U2612
J. Abel	M7047Q
L. Carter	M7047Q
S. Kaplan	U7026
J. Mirabal	U7026
Y. Yu	U7026
D. Rosard	U7026
J. R. Freelin	U2612
M. Gaitens	U2612
A. Sims	U4632
E. Fried	M2101
R. Peck	M2101
K. Folgate	U4633
R. Hinrichs (10 copies)	U4633
J. Guy	M4214
W. Granat	M4214
R. Karcher	M4214
C. Mayforth	U2704
S. Schmidt (6 copies)	U2704
H. Foulke (6 copies)	U2513
P. Weygandt	U2420
Dr. Puri	U4424
R. P. Wanger	U2513

MSD Library (1 Reproducible Master and 10 Copies)

Technical Data Center (2 Copies and 6 Title Pages)
General Electric Company
Building #5
Schenectady, New York